FACTA UNIVERSITATIS (NIŠ)
Ser. Math. Inform. Vol. 30, No 3 (2015), 353–359

APPLICATIONS OF THE MEAN CURVATURE FLOW ASSOCIATED TO ANISOTROPIC GENERALIZED LAGRANGE METRICS IN IMAGE PROCESSING

Vladimir Balan and Jelena Stojanov

Abstract. The Geodesic Active Field (GAF) approach from image processing - whose mathematical background is the Riemannian theory of submanifolds - was recently extended by the authors to the Finslerian setting, for certain specific metrics of Randers type. The present work studies the significantly more flexible Generalized Lagrange (GL) extensions, which allow a versatile adapting of the GAF process to Finslerian, pseudo-Finslerian and Lagrangian structures. The GAF mean curvature flow PDEs of three such GL structures (Randers-Ingarden, Synge-Beil, and proper Generalized Lagrange) are explicitly obtained, discussed, implemented, and their corresponding feature evolutions are compared with the classic results produced by the established original Riemannian GAF model.
Keywords: The Geodesic Active Field; Riemannian manifold; Image processing; Generalized Lagrange metrics.

1. Introduction. Related works.

The Beltrami framework and its practical importance in image processing were extensively described in [5, 11, 14, 15]. Applications to image segmentation, edge detection, denoising and stereo vision were achieved by means of a flow technique, which evolves surfaces associated to digital images. The related surface evolution details are comprehensively presented in [10, 12].

A curve evolution technique, called geodesic active contours (GAC) is used in image segmentation [6]. As a natural extension, the geodesic active field (GAF) framework for image registration was introduced in [16], and further improved in [17]. The GAF technique is based on minimization of the deformation field between a pair of images. It evolves a surface corresponding to the deformation field to achieve the minimality of a weighted Polyakov action [5], by employing the mean curvature (*MC*) flow. The weighted Polyakov action minimization in the

Received September 02, 2014; Accepted March 02, 2015
2010 *Mathematics Subject Classification.* Primary 53B40; Secondary 53C60, 53C44

Riemannian type framework is achieved by the Beltrami PDE flow - an isotropic (directional independent) evolutive equation of a 2-dimensional geometric active object.

On the other hand, [9] and [13] promote anisotropic extensions of geodesic active contours. They consider a curve as 1-dimensional geometric active object, and use anisotropic weighted curve length for segmentation and for curve extraction, respectively. The non-weighted anisotropic evolution of image surfaces was recently proposed in [1], where an approximate minimizing flow contains only the most significant term from the scaled extremal equation. The present work relies on the general anisotropic Beltrami framework, which was recently developed by the authors in [2]; it discusses as well discretization and applicable aspects of the obtained theoretical results.

2. Beltrami framework and anisotropic extension

The central object of a Beltrami framework is a surface embedded into a Riemannian manifold, and its evolution in accordance with the minimization of a global scalar property of the surface, expressed as a Poyakov action. Let us consider the embedding map

$$X : D \to M, \quad (\dim D = n < \dim M = m). \tag{2.1}$$

The embedding produces the submanifold $\Sigma = X(D)$ of the Riemannian manifold (M, h), usually called *the image surface*. This is endowed with a Riemannian metric g, which is not necessarily induced from h. The preliminary aim is to describe the evolution of the image surface (Σ, g) towards the extreme state of the minimal Polyakov action $S(X, g, h, f) = \int L\, dx^1 \dots dx^n$ defined by the Lagrangian density

$$L = f(X, g, h) \cdot g^{\mu\nu} \frac{\partial X^i}{\partial x^\mu} \frac{\partial X^j}{\partial x^\nu} h_{ij} \sqrt{g}, \tag{2.2}$$

where we denote by f the weight function and by g the determinant of the metric tensor $(g_{\mu\nu})$.

We shall further briefly denote, for a given function Φ:

$$\Phi_{;\alpha} := \frac{\partial \Phi}{\partial x^\alpha} \qquad \Phi_{,i} := \frac{\partial \Phi}{\partial X^i} \qquad \Phi_{,\binom{i}{\alpha}} := \frac{\partial \Phi}{\partial X^i_\alpha}.$$

The Euler-Lagrange equation

$$\partial_t X^r = -\frac{1}{2} \frac{1}{\sqrt{\gamma}} h^{ir} \left(L_{,i} - L_{,\binom{i}{\alpha};\alpha} \right) \tag{2.3}$$

yields the descent flow, called *the Beltrami flow*

$$\partial X^r_t = f \tau^r(X) - \frac{n}{2} f_{,i}\, h^{ir} + f_{,i}\, g^{\sigma\mu} X^i_\sigma X^r_\mu, \tag{2.4}$$

where $\tau^r(X)$ is the tension field associated to the embedding,

$$\tau^r(X) = g^{\alpha\sigma} X^r_{\alpha\sigma} - g^{\rho\theta}\Gamma^{\sigma}_{\rho\theta} X^r_{\sigma} + g^{\sigma\mu}\Gamma^r_{kl} X^k_{\sigma} X^l_{\mu}. \tag{2.5}$$

The main benefits of the Beltrami framework and of the resulting flow, are the arbitrary and independent choices of g and h, the possibility of considering the vector value feature, and the geometrical quality of the flow (its reparametrization invariance).

The various choices of metric g and the weight function f yield different flows:

mean curvature flow, $\partial_t X^r = H^r$:	g -induced, $f \equiv 1$;
tension flow, $\partial_t X^r = \tau^r$:	$g = g(x)$ -arbitrary, $f \equiv 1$;
Beltrami flow, $\partial_t X^r = \partial_t X^r(x)$:	$g = g(x)$ -arbitrary;
anisotropic flow, $\partial_t X^r = \partial_t X^r(x, v)$:	$g = g(x, v)$ -directionally dependent.

In the last case - the anisotropic Beltrami framework - the image metric is a smooth tensor field on the tangent bundle $T\Sigma$. In order to distinguish it from the used Riemannian type metrics, we denote this with Greek letters, $\gamma = \gamma_{\mu\nu} dx^{\mu} \otimes dx^{\nu}$. If the metric γ is symmetric, regular and of constant signature, then (Σ, γ) is a generalized Lagrange space [4], and the anisotropic Beltrami flow ensuring the minimal Polyakov action is briefly called the *GL* flow. Its explicit form is developed in [2].

Theorem 2.1. *(The anisotropic Beltrami flow) Let γ be a generalized Lagrange metric on the surface embedded via (2.1) into the Riemannian manifold (M, h). The PDE of the anisotropic Beltrami flow which provides the minimality of the non-weighted Polyakov action on the surface (Σ, γ), is*

$$\begin{aligned}
\partial_t X^r = {} & \tau^r(X) \\
& + \frac{1}{2} h^{ir} \Big\{ g_{\sigma\mu;\alpha} \Big[(\gamma^{\sigma\mu})_{,\binom{i}{\alpha}} + \gamma^{\sigma\mu} (\ln \sqrt{\gamma})_{,\binom{i}{\alpha}} \Big] + \\
& \quad g_{\sigma\mu} \Big[(\gamma^{\sigma\mu})_{,\binom{i}{\alpha};\alpha} + (\gamma^{\sigma\mu})_{,\binom{i}{\alpha}} (\ln \sqrt{\gamma})_{;\alpha} + (\gamma^{\sigma\mu})_{;\alpha} (\ln \sqrt{\gamma})_{,\binom{i}{\alpha}} \\
& \quad + \gamma^{\sigma\mu} \tfrac{1}{\sqrt{\gamma}} (\sqrt{\gamma})_{,\binom{i}{\alpha};\alpha} - (\gamma^{\sigma\mu})_{,i} - \gamma^{\sigma\mu} (\ln \sqrt{\gamma})_{,i} \Big] \Big\},
\end{aligned}$$

where $g_{\mu\nu} = h_{ij} \partial_{\mu} X^i \partial_{\nu} X^j$ is the induced metric on the embedded surface.

Without losing the generality, one can consider for the anisotropic metric γ, the deformed induced one

$$\gamma_{\mu\nu}(x, v) = g_{\mu\nu}(x) + \varphi_{\mu\nu}(x, v), \quad x \in \Sigma, v \in T_x\Sigma.$$

If the embedded surface is endowed with a Finsler structure $F : T\Sigma \to \mathbb{R}$ [3, 8], then the anisotropic metric is defined by the halved Hessian

$$\gamma_{\mu\nu}(x, v) = \frac{1}{2} \frac{\partial^2 F^2}{\partial v^{\mu} \partial v^{\nu}} \Big|_{(x,v)}.$$

A particular linearly deformed induced norm is the one of Randers type [3, 8, 7],

$$F(x,v) = \sqrt{g_{\mu\nu(x)}v^\mu v^\nu} + b_\mu(x)v^\mu;$$

in this case, the corresponding Beltrami flow is ([2]),

$$\partial_t^R(X^r) = \tau^r(X) + \phi(g_{\mu\nu}(x), b_\mu(x), \|v\|_g). \tag{2.6}$$

As well, for Σ endowed with a generalized Lagrange structure of Synge-Beil type,

$$\gamma_{\mu\nu}(x,v) = g_{\mu\nu}(x) + c(X)v_\mu v_\nu,$$

having the covariant directional vector $(v_\mu) = (g_{\mu\nu}v^\nu)$, Theorem 2.1 produces the Synge-Beil type Beltrami flow,

$$\partial_t^{SB}(X^r) = \tau^r(X) + \psi(g_{\mu\nu}(x), c(X), \|v\|_g). \tag{2.7}$$

3. The Beltrami framework in image processing

The Beltrami framework commonly used in image processing mainly considers a Monge surface in the 3-dimensional Euclidean space $X : D \to M$, where $(M, h) = (\mathbb{R}^3, h_{ij} = \mathrm{diag}(1, 1, \beta^2))$,

$$X : (x^1, x^2) \mapsto (x^1, x^2, I(x^1, x^2)).$$

The components of the induced metric on the surface are

$$(g_{\mu\nu}) = \begin{pmatrix} 1 + \beta^2 I_{x^1}^2 & \beta^2 I_{x^1} I_{x^2} \\ \beta^2 I_{x^1} I_{x^2} & 1 + \beta^2 I_{x^2}^2 \end{pmatrix},$$

where, for brevity, we use the notation $I_{x^\mu} = \frac{\partial I}{\partial x^\mu}$.

The gradient vector field $gradI = (g^{1\alpha}I_{x^\alpha}, g^{2\alpha}I_{x^\alpha})$ is an ingredient for constructing the following Finslerian norm of Randers-Ingarden type ([3]):

$$F(x,v) = \sqrt{g_{\mu\nu}v^\mu v^\nu} + I_{x^\mu}v^\mu, \tag{3.1}$$

where $b_\mu = I_{x^\mu}$ is the term which characterizes the Ingarden structure. Further, the Finslerian-Randers type metric components and the PDE of the evolution flow can be calculated, and only the third component of the flow, $\partial_t X^3 = \partial_t I$ is nontrivial. This allows to derive the flow $\partial_t^R I$ for the Monge surface evolution (2.6).

Theorem 2.1 and the Synge-Beil structure given on the Monge surface,

$$\gamma_{\mu\nu}(x,v) = g_{\mu\nu}(x) + v_\mu v_\nu, \tag{3.2}$$

yield the corresponding flow $\partial_t^{SB} I$ (2.7).

We note that this extends the isotropic Beltrami flow used in [16], which coincides with the mean curvature flow, $\partial_t I = H^3$.

4. Application and tentative implementation

A grayscale image is viewed as a matrix $\Sigma = (I(i,j))$, whose elements express the greyness of pixels:

$$x = (x^1, x^2) = (i, j) - \text{ matrix position,} \qquad I(i,j) \in \{0, 1, \dots, 255\},$$

where the tangent vectors point to the neighboring pixels characterized by the displacements

$$v(i,j) = (v^1, v^2) \in \{(-1,-1), (-1,0), (-1,1), (0,-1), (0,1), (1,-1), (1,0), (1,1)\}.$$

The evolution is achieved by the successive shifting of the grayscale image

$$I(i,j) \to I(i,j) + \triangle I(i,j), \tag{4.1}$$

where $\triangle I(i,j)$ discretizes one of the following flow types: Randers-Ingarden, Synge-Beil or mean curvature.

We use Matlab programming for implementing the three Beltrami flows. The corresponding Beltrami evolutions (4.1) are achieved by successive shifting, where each iteration assumes the following steps:

- accessing pixel (except of the boundary) to get the corresponding feature value;
- determining the shift tangent vector - optionally, in the cases of anisotropic flows;
- applying the flow expression on the feature value and optionally on the shift tangent vector to obtain the shift value $\triangle I$;
- computing the modified feature value, $I \to I + \triangle I$.

The main difference between the implementation of isotropic and anisotropic evolution types is in the dependence - in the latter case - of the metric on the eight discretized neighboring Gateaux derivatives at each pixel position. Namely, the anisotropic flows exhibit the extra local dependence of the norm and hence metric tensor on the eight neighbors as well, compared to dependence on position only, present in the isotropic flow. In our research point, the gradient is taken for the anisotropic shift.

Due to technical limitations, low resolution images were considered for processing. The shifting was achieved for $\beta = 2$, by the use of the Randers-Ingarden flow $\partial_t^R I$ given by (2.6)-(3.1), the Synge-Beil flow $\partial_t^{SB} I$ from (2.7)-(3.2), and the classical mean curvature flow

$$\partial_t^{MC} I = \frac{1}{g^2}\left(I_{x^1x^1} g_{22} + I_{x^2x^2} g_{11} - 2 I_{x^1x^2} g_{12}\right).$$

The applicative aspects of the research currently emphasize the construction of the shift matrices $\triangle I = (\triangle I(i,j))$ and the low resolution is a limiting factor in visualizing immediate enhancement of the starting image as effect of the flow action.

The Randers-Ingarden evolution sample obtained after 15 iterations can be seen in Figure (4.1). The effects of the preliminarily implementations can be tracked by means of the shift matrices corresponding to the three flows.

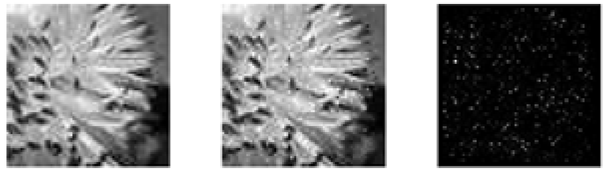

FIG. 4.1: Original flower image (60×60), the 16-th *RI* iteration output, and the latter flow-shift.

5. Conclusions and further developments

The obtained preliminary results show that for all the three considered flows, the output differs from the input by a slight increase of contrast between compact regions of the image. The anisotropic evolutions need extra computational resources than the mean curvature one, due to the complexity of the anisotropic flow expressions compared to the *MC* flow. However, though the directional dependence slows down the speed of the enhancement process, it has the merit of considerably enabling its sensitivity. Due to their extended local character, the anisotropic flows provide more information than the Riemannian ones, and aim to simplify the further intended processing of the output features.

Further concerns of the subject will address the optimal adapted selection of the direction-dependent anisotropic structure, and will consider a non-constant weight function within the Polyakov energy, which tunes the evolution shift, and accelerates the image enhancement.

REFERENCES

1. V. BALAN, J. STOJANOV, *Finslerian extensions of geodesic active fields for digital image registration*, Proceedings in Applied Mathematics and Mechanics / PAMM, 13, 1, 2013, pp. 493–494.
2. V. BALAN, J. STOJANOV, *Finslerian-type GAF extensions of the Riemannian frameworkin digital image processing* , to appear.
3. D. BAO, S.-S. CHERN AND Z. SHEN, *An Introduction to Riemann-Finsler Geometry*, Graduate Texts in Mathematics, Volume 200, Springer-Verlag, 2000.
4. I. BUCATARU, R. MIRON, *Finsler-Lagrange geometry. Applications to Dynamical Systems*, Ed. Acad. Romane, Bucharest, 2007.
5. X. BRESSON, P. VANNDERGHEYNST J.P. THIRAN, *Multiscale Active Contours*, Int. Jour. of Comp. Vision **70**(3) (2006), 197–211.
6. V. CASELLES, R. KIMMEL, G. SAPIRO, *Geodesic active contours*, Int. Jour. of Comp. Vision **22**(1) (1997), 61–79.

7. X. Cheng, Z. Shen, *Finsler Geometry: An approach via Randers Spaces*, Science Press & Springer, 2012.
8. S.-S. Chern and Z. Shen, *Riemann-Finsler Geometry*, World Sci. Publishers, 2005.
9. G. Gallego, J.I. Ronda and A. Valdes, *Directional geodesic active contours*, 19th IEEE International Conference on Image Processing (ICIP), September 30 - October 3, Orlando, FL, USA, 2012, pp. 2561–2564.
10. Y. Giga, *Surface evolution equations: a level set method*, Hokkaido University Technical Report Series in Mathematics No. 71, 2002.
11. R. Kimmel and R. Malladi and N. Sochen, *Images as embedded maps and minimal surfaces: movies, color, texture, and volumetric medical images*, Int. Journal of Comp. Vision **39**(2) (2000), 111–129.
12. R. Kimmel, *Numerical Geometry of Images*, Springer-Verlag, New York 2004.
13. J. Melonakos, E. Pichon, S. Angenent and A. Tannenbaum, *Finsler active contours*, IEEE Trans. on Pattern Analysis and Machine Intelligence **30**(3) (2008), 412–423.
14. N. Sochen and R. Deriche and L.-L. Perez, *The Beltrami flow over manifolds*, Technical Report No 4897, Sophia Antipolis Cedex, INRIA, France 2003.
15. N. Sochen and R. Kimmel and R. Malladi, *A general framework for low level vision*, IEEE Trans. on Image Processing **7**3 (1998), 310–318.
16. D. Zosso, X. Bresson and J.-P. Thiran, *Geodesic active fields - a geometric framework for image registration*, IEEE Trans. on Image Processing **20**(5) (2011), 1300–1312.
17. D. Zosso, X. Bresson, J.-P. Thiran, *Fast Geodesic Active Fields for Image Registration Based on Splitting and Augmented Lagrangian Approaches*, Image Processing, IEEE Transactions on , **23**(2) (2014), 673–683.

Vladimir Balan
Faculty of Applied Sciences
Department Mathematics-Informatics
Univ. Politehnica of Bucharest
Romania
vladimir.balan@upb.ro

Jelena Stojanov
Technical Faculty ”Mihajlo Pupin”
University of Novi Sad
23000 Zrenjanin, Serbia
stojanov.jelena@gmail.com